

Estimating light-use efficiency by the separated Solar-induced chlorophyll fluorescence from canopy spectral data

CHENG Zhanhui^{1,2}, LIU Liangyun¹

1. Center for Earth Observation and Digital Earth, Chinese Academy of Sciences, Beijing 100190, China;

2. College of Information and Electrical Engineering, China Agriculture University, Beijing 100083, China

Abstract: Light-use efficiency (LUE) is a critical parameter in many primary production models for estimating ecosystem carbon exchange. The application of these models on regional and global scale is restricted because of the difficulty of retrieving LUE from airborne and satellite remote sensing images. Vegetation chlorophyll fluorescence is a direct indicator of plant physiology. In this paper, a diurnal experiment was carried on maize on July 5, 2008. The canopy radiance spectra and tower-based flux data were acquired synchronously to test the possibility of retrieving LUE by the solar-induced vegetation ChlF signals. The canopy net primary production (NEP) values were calculated using eddy covariance measurement by a CSAT3-Li7500 Flux system, and the gross primary production (GPP) was also calculated by adding the simulated day time respiration. Two kinds of LUE based on GPP (LUE_{GPP}) and NEP (LUE_{NEP}) were defined by dividing the absorbed photosynthetic active radiation (APAR). The ChlF signals at 760nm and 688nm were also separated from the reflected radiance spectra based on Fraunhofer line depth algorithm in the two oxygen absorption bands. The ChlF signals were strongly correlated with photosynthetic active radiation (PAR), especially the ChlF at 760nm ($R^2 > 0.99$). Both NEP and GPP had a significant correlation with ChlF. Furthermore, LUE_{GPP} was negatively correlated with the ChlF's relative intensity at 688nm and 760nm, with a correlation coefficient R^2 of 0.6331 and 0.7861 respectively. Moreover, the LUE models based on the solar-induced vegetation ChlF signals were compared to some popular vegetation Indices (VIs) from the canopy reflected spectra. Canopy LUE_{GPP} was proved able to be estimated from the remotely sensed ChlF signals.

Key words: spectra, chlorophyll fluorescence, light-use efficiency (LUE), primary production

CLC number: TP79 **Document code:** A

Citation format: Cheng Z H and Liu L Y. 2010. Estimating light-use efficiency by the separated Solar-induced chlorophyll fluorescence from canopy spectral data. *Journal of Remote Sensing*. 14(2): 356—371

1 INTRODUCTION

Terrestrial ecosystems can fix about 60Gt of carbon annually through the physiological process of photosynthesis. Meanwhile, autotrophic and heterotrophic respirations on the earth's surface release about the same amount of carbon back into the atmosphere thereby closing the terrestrial carbon cycle (Janzen, 2004). Even tiny alterations in the terrestrial carbon balance are likely to cause significant change on atmospheric CO₂ concentrations. For this reason, the estimation of land-atmosphere carbon cycle is becoming a focus in the research of global climate change. Among most of the productivity models, only the models based on light-use efficiency (LUE) are widely used in regional and global vegetation productivity estimation, because of their advantages of simplicity in calculation and less input parameters (Potter *et al.*, 1993; Running *et al.*, 1999; Xiao *et al.*, 2005; Hilker *et al.*, 2008).

LUE is a critical parameter in the primary production models, which can be defined as the efficiency of plant converting absorbed light energy into dry matter. At regional or global scale, LUE can only be estimated by prior parameters, such as land cover types, light, temperature and water status retrieved from remote sensing or in situ measurements. Therefore, the development of the LUE based productivity models is limited. So far, the Eddy covariance (EC) technique is the only way to measure carbon dioxide and water-heat exchange between atmosphere and vegetation canopy directly. This method can acquire LUE on canopy or landscape scale, and verify the remote sensing production estimation on regional scale.

Light absorbed by a leaf can be dissipated as heat, or used for photochemistry, or emitted as fluorescence, there is a reciprocal relationship among three of them. Chlorophyll fluorescence (ChlF) is considered as an ideal probe of photosynthetic activity because of the characteristics of rapid and non-invasive

Received: 2009-01-05; **Accepted:** 2009-05-01

Foundation: National Basic Research Program of China (973 Program) (No. 2009CB723902), the National Natural Science Foundation of China (No. 40771134), and the National High Tech R&D Program of China (No. 2006AA10Z201).

First author biography: CHENG Zhanhui(1986—), female, postgraduate. Research fields: quantitative remote sensing of vegetation. E-mail: zhanhui-cheng@163.com

Corresponding author: LIU Liangyun, E-mail: lyliu@ceode.ac.cn

reflection of plant photosynthesis state (Schreiber, 1994). Therefore, it can be used to monitor instantaneous vegetation Light-use efficiency. The observed apparent vegetation reflectance signal includes contributions from both reflected and fluoresced radiations. Although the intensity of the ChlF emission is relatively low, many researches (Moya *et al.*, 2004; Liu *et al.*, 2005; Louis *et al.*, 2005; Liu *et al.*, 2006) proved it possible to separate solar-induced ChlF radiation from observed apparent vegetation reflectance by Fraunhofer Line Detection (FLD) algorithm. So far, most researches mainly focus on active fluorescence detection of photosynthetic activity, while research on passive fluorescence detection of photosynthetic activity is still at the preliminary stage. Therefore, a diurnal change experiment was carried out to test possibility of retrieve LUE from the solar-induced ChlF signals. Canopy ChlF signals were calculated from the canopy radiance spectra, and also the canopy LUE was retrieved synchronously from carbon dioxide flux measured by Eddy covariance (EC) method. Based on the statistical relations between ChlF signals and primary productivity parameters, the feasibility of detecting canopy LUE by vegetation ChlF was discussed, which may be a reliable remote sensing approach to retrieve LUE on canopy and regional scale.

2 MATERIALS AND METHODS

2.1 Experimental designs

A diurnal change experiment was designed for summer maize to acquire the canopy-level spectra, radiation and CO₂ flux values. The experiment was performed on July 5 2008 at Yingke Irrigation Area, Zhangye, Gansu Province (38.85° N, 100.41° E), and the maize was at the big trumpet period with a mean height of 1.76m. The vegetation coverage was about 95% measured from canopy digital photo with the algorithm described in Li *et al.* (2004). The experimental field had normal fertilizer management and uniform growth, and its size was about 3.3×10^4 m². And an eddy flux tower was fixed in the center of the field. The day was sunny and clear, with the photosynthetic active radiation (PAR) around 200—2000 $\mu\text{mol m}^{-2} \text{s}^{-1}$ and wind speed less than 1.5m s⁻¹.

2.2 Canopy spectra data

The canopy spectral measurements were taken from the canopy using an ASD FieldSpec FR spectrometer. All the canopy and panel radiance spectra were taken every 60 min from 10:00 to 16:00 and every 30 min from 16:00 to 20:00. The spectrometer was fitted with a 25° field-of-view bare fiber-optic cable, and operated in the 350—2500 nm spectral region with a sampling interval of 1.4 nm between 350 and 1050 nm and 2 nm between 1050 and 2500 nm. The spectral resolution (or FWHM) was 3 nm for the 350—1000 nm region and 10 nm for the 1000—2500 nm region. As shown in Fig.1, the fiber optics was fixed at the southern end of a north-south direction hori-

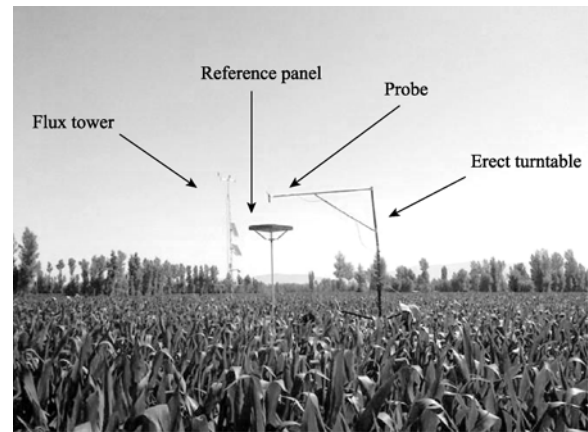


Fig. 1 Photo of detecting canopy spectrum

zontal pole, which was fixed by an erect turntable. All canopy spectra were taken 2.3 m above the canopy. A 0.5m × 0.5m BaSO₄ panel was selected as the calibration reference with a reflectance about 45% in visible and near-infrared region. The reference panel was raised horizontally by another vertical pole with center almost 0.5m right under the optical probe when it was measured. Radiance observation pattern was adopted for the field spectrometer in this experiment. Each spectrum was averaged from 10 individual measurements of the maize target. Then, the spectrometer was quickly rotated 180 degrees right above the reference panel to measure the panel radiance spectrum.

2.3 Radiometric measurements

The photosynthetic active radiation (PAR) was measured with a SunScan Canopy Analysis System (Delta Inc., England). The sensor was held toward the south and kept horizontal using an air bubble beside the handset controller. Four parts of PAR was measured in this experiment: the incident PAR (PAR_i), the canopy reflected PAR (PAR_r), the canopy transmitted PAR (PAR_t) and the PAR reflected by the soil background (PAR_g), both the PAR_i and PAR_r were taken at a height of 20 cm above the canopy. Three representative positions were chosen to acquire PAR_i, PAR_r, PAR_t and PAR_g respectively, and the average absorbed photosynthetically active radiation (APAR) was calculated as follows (Jenkins *et al.*, 2007),

$$\text{APAR} = \text{PAR}_i - \text{PAR}_r - \text{PAR}_t + \text{PAR}_g \quad (1)$$

2.4 Flux and meteorological data

An Eddy covariance system and a DYNAMET Weather Station were installed in the field to acquire meteorological data, and to measure the materials and energy exchange between canopy and atmosphere.

This EC tower consisted of a fast-response 3D sonic anemometer (CSAT3, Campbell Scientific Inc., USA) and an open-path gas analyzer (LI-7500, Li-Cor Inc., USA) with data recorded at 10Hz and fluxes such as CO₂, latent heat, sensible

heat and momentum calculated every 30 min. A positive flux value indicates a direction of material propagation was upward. Before 30 min productions were produced, WPL corrections were applied (Webb *et al.*, 1980), and abnormal data caused by instrument malfunctions or sudden changes in the weather was deleted. The DYNAMET Weather Station fixed at the tower was used to record the weather parameters, such as PAR, temperature, rain, and winds every 10 min.

3 RESULTS AND ANALYSIS

3.1 Extraction of Canopy ChlF

The emitted chlorophyll fluorescence, mixed by vegetation reflection of incident sunlight, only accounts for less than 3% of the apparent reflectance light energy (Grace *et al.*, 2007). Therefore, it is important to find an effective way to extract the tiny ChlF signal from the apparent reflectance spectrum. The simple and feasible chlorophyll fluorescence spectrum separation algorithm based on Fraunhofer Line principles had been successfully applied in some researches on emission ChlF spectrum at certain wavelengths (Moya *et al.*, 2004; Liu *et al.*, 2005; Louis *et al.*, 2005; Liu *et al.*, 2006). Evain *et al.* (2001), Moya *et al.* (2004) even developed fluorescence spectrum detection instrumentation based on Fraunhofer Line principles.

The tiny dark absorption lines in the spectrum of the sun, caused by atmospheric absorption of the sun and the earth, are called Fraunhofer Lines. Its FWHM is commonly between 0.1 nm and 10 nm, such as 486 nm, 527 nm, 589 nm, 688 nm and 760 nm. The idea of ChlF spectral separation algorithm supposes that the reflectance is stable around the Fraunhofer lines and vegetation emitted ChlF can fill the Fraunhofer "well" to a certain degree. Therefore, vegetation ChlF radiance can be extracted by comparison of incident solar radiance and vegetation reflected radiance in certain wavelengths. The ChlF (f) was calculated as follows,

$$f = \frac{a \times d - c \times b}{a - b} \quad (2)$$

where a and b represent the detected irradiance from the reference panel in and out of the oxygen-absorption feature. Similarly, c and d represent the detected radiance from the target at the border and at the bottom of the band. Not only the ChlF but also the relative ChlF (R-ChlF, f^*) can be extracted from the reflectance spectrum. According to Eq. (2), the R-ChlF can be calculated as,

$$f^* (\%) = \frac{f}{a} \times 100 = \frac{ad - cb}{a^2 - ab} \times 100 \quad (3)$$

Liu *et al.* (2006) successfully extracted vegetation ChlF spectrum at 688 nm and 760 nm bands with ASD spectrometer by Eq. (2) and Eq. (3), which confirmed the feasibility to extract vegetation ChlF spectrum by this ChlF spectrum separation algorithm.

The ChlF's diurnal change curves of summer maize (C4 plant) at 688 nm and 760 nm wavelength were shown in Fig.2, which demonstrated a characteristic of higher intensity at noon than that at morning and evening. Moreover ChlF intensity at 688 nm band was significantly higher than that at 760 nm band. This result was different from Liu *et al.* (2006)'s study on winter wheat (C3 plant), but the same as the study on ivy (C4 plant) (Liu *et al.*, 2006). This indicates different physiological mechanism of photosynthesis for the C3 and C4 plant functional types. However, no reliable interpretation was found to interpret the relationship between the different photosynthesis ways and fluorescence yield.

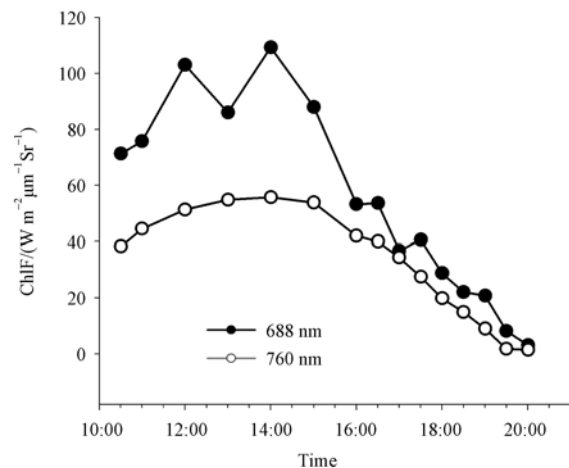


Fig. 2 Diurnal changes of chlorophyll fluorescence (ChlF) at 688nm and 760nm

When the target remains stable, ChlF intensity is mainly affected by environment variations, mostly by the incident PAR. The correlation between the solar-induced ChlF radiation and PAR given in Fig.3 showed the positive linear correlations at 688 nm and 760 nm, with a correlation coefficient (R^2) of 0.8874 and 0.9938, respectively. The result favored the self-protective mechanism of ChlF at high irradiance level. Plant would convert more light energy into fluorescence when the incident light was stronger, to avoid damage to vegetation photosynthetic organs under high incident light intensity. Some researches (Dobrowski *et al.*, 2005; Louis *et al.*, 2005) showed that ChlF at 688 nm would be absorbed by chlorophyll again. This might be the reason for lower correlation coefficients of ChlF and PAR at 688 nm than that at 760 nm (Fig.3).

3.2 Vegetation primary productivity and ChlF

3.2.1 NEP

The ecosystem-atmosphere CO_2 flux (net ecosystem exchange, NEE) was measured with an eddy covariance system, which was negative when CO_2 was diffused from the atmosphere into the ecosystem. NEE shared the same absolute value with net ecosystem production (NEP) but the opposite symbol,

$$\text{NEP} = -\text{NEE} \quad (4)$$

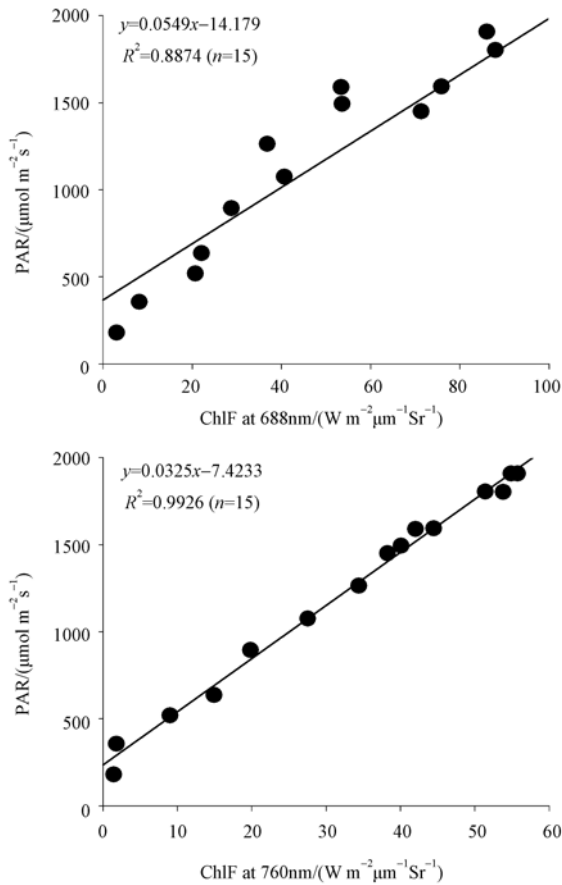


Fig. 3 Relationship between PAR and chlorophyll fluorescence at 688nm and 760nm

In this experiment, NEP and solar-induced ChlF were mainly affected by environmental conditions. Fig.4 showed a positive linear correlation between NEP and the separated ChlF at 688 nm and 760 nm with the correlation coefficients (R^2) to be 0.7552 and 0.9092 respectively. The result suggested that both solar-induced ChlF and NEP had the same response for the short-term environmental change; and NEP short-term changes could be retrieved from vegetation emitted ChlF.

3.2.2 GPP

Nighttime NEE acquired by EC system represents nighttime ecosystem respiration (RE) because plants do not photosynthesize at night. Many researches have proved that nighttime NEE can be described by an exponential function of temperature (Lloyd and Taylor, 1994; Nichol *et al.*, 2000; Wang *et al.*, 2004; Zhang *et al.*, 2007). Soil temperatures were measured at different depth and variance of ecosystem respiration was generally explained by air temperature (Reichstein *et al.*, 2005). Hence, 2m height air temperature measured by weather station instead of average air temperature (T_a) was used as input for the RE-T empirical formula. The expression was described as follows,

$$RE = Ae^{BT_a} \quad (5)$$

where A and B are constants determined from nighttime T_a and CO_2 flux data (namely NEE). Daytime RE can be evaluated with Eq. (5) under the assumption that daytime RE response

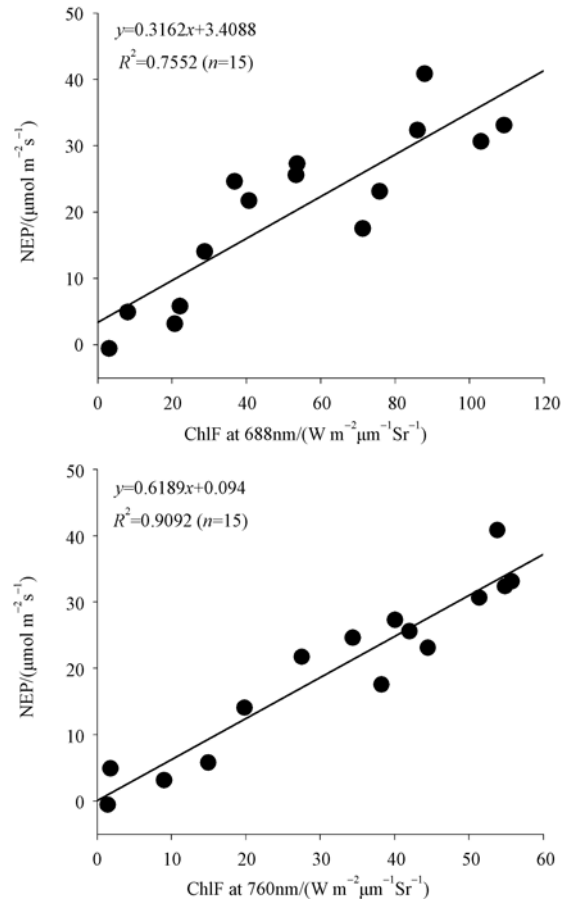


Fig. 4 Relationship between NEP and chlorophyll fluorescence at 688nm and 760nm

to T_a is identical with nighttime (Zhang *et al.*, 2007). Some researches reported that the RE measured by the eddy covariance method was significantly lower than the true value (Goulden *et al.*, 1996; Law *et al.*, 1999). To minimize the bias, only those NEE data from periods of high friction velocity ($u^* > 0.15 \text{ m s}^{-1}$) were used as nighttime respiration (Zhang *et al.*, 2007). So, only 30% of nighttime data between 2008-07-04 and 2008-07-09 were used in daytime RE estimation. A and B , calculated by nighttime data, was 2.8898 and 0.0591 respectively ($R^2=0.4703$, $n=15$). Then, the daytime RE values were calculated from Eq. (5).

The impact of ecosystem respiration on carbon exchange was distinctive among different ecosystems. However, gross primary production (GPP) represents the total carbon fixed by photochemical reaction without any respiration, and can be expressed as Eq. (6) (Wang *et al.*, 2004; Yuan *et al.*, 2007; Coops *et al.*, 2007),

$$GPP = NEP + RE \quad (6)$$

Diurnal changes of NEP, GPP and RE were shown in Fig. 5. RE accounted for 30% of GPP all day, and reached to 77% and 100% at morning and evening respectively. The integral of all

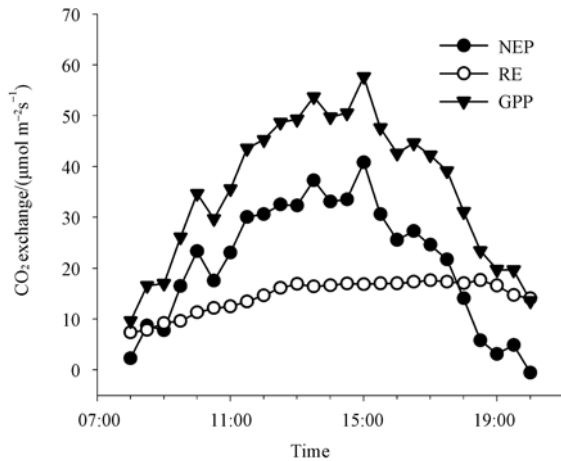


Fig. 5 Diurnal changes of net ecosystem production (NEP), gross primary production (GPP) and ecosystem respiration (RE)

day GPP:NEP:RE equaled to 0.5:0.3:0.2. These results showed that RE value can not be ignored in vegetation GPP and NEP estimation. Especially, after 18:00, NEP dropped to zero due to low light irradiance, while the GPP still kept around $13.58 \mu\text{mol m}^{-2} \text{s}^{-1}$ because of persistent high temperature. Autotrophic respiration was preponderating at this time, organic carbon created by photosynthesis was not sufficient to counteract ecosystem respiration.

ChlF emissions of vegetation canopies are indicative of leaf photosynthesis condition, and insignificant to respiration. Thus, it would be reasonable to establish reliable relationship between canopy solar-induced ChlF and vegetation GPP. Fig.6 showed a positive linear correlation between GPP and the separated ChlF at 688 nm and 760 nm with the correlation coefficients (R^2) to be 0.6688 and 0.8514 respectively.

Fig. 4 and Fig. 6 showed that vegetation ChlF was significantly positive correlated with both NEP and GPP, especially R^2 at 760nm were above 0.85. The results showed ChlF can be used in vegetation LUE detection.

3.3 LUE and relative ChlF

Commonly, light-use efficiency (LUE) can be calculated as follows,

$$\text{LUE}(\%) = \frac{P}{\text{APAR}} \times 100 \quad (7)$$

where, APAR is calculated from Eq. (1), P is varied with the different export parameters of LUE models. Utilizing flux measurement data, the LUE is calculated based on NEP (LUE_{NEP}) and GPP (LUE_{GPP}) respectively,

$$\begin{aligned} \text{LUE}_{\text{NEP}}(\%) &= \frac{\text{NEP}}{\text{APAR}} \times 100 \\ \text{LUE}_{\text{GPP}}(\%) &= \frac{\text{GPP}}{\text{APAR}} \times 100 \end{aligned} \quad (8)$$

Both ChlF emissions of vegetation and GPP are direct production of photosynthesis process. ChlF is irrelevant to vegetation

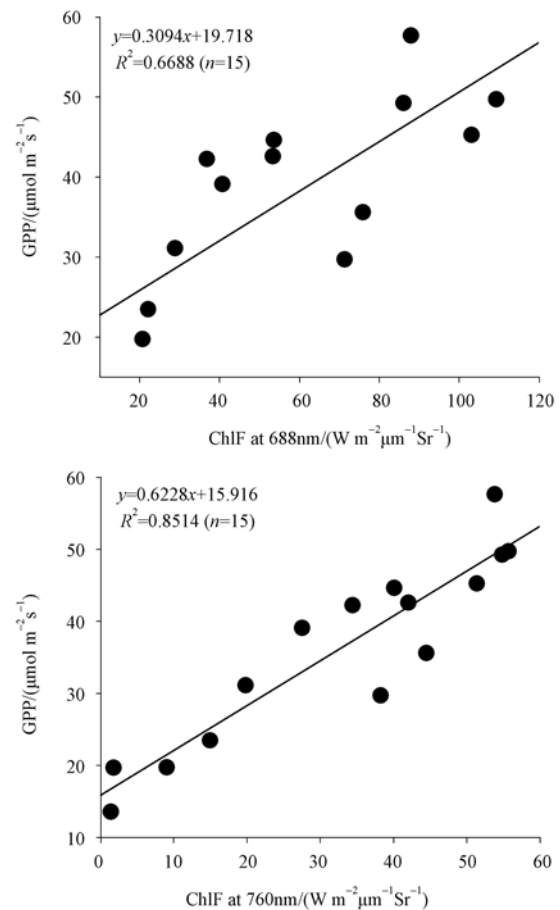


Fig. 6 Relationship between GPP and chlorophyll fluorescence at 688nm and 760nm

autotrophic respiration. Taking the total organic carbon fixed by photochemical reaction as an input of the LUE model can compensate the ecosystem respiration dissipation of the photosynthetic carbon fixation. The physical mechanism between ChlF and LUE_{GPP} is more directly, and LUE_{GPP} and LUE_{NEP} were calculated respectively according to Eq. (8).

Consistent with LUE conception, the R-ChlF defined in Eq. (3) is sensitive to diurnal changes of vegetation LUE. The relationship between the R-ChlF and LUE_{GPP} was given in Fig.7. The figure showed a negative correlation between LUE_{GPP} and R-ChlF at 688 nm and 760 nm with the correlation coefficients (R^2) to be 0.6331 and 0.7861 respectively. Higher R-ChlF led to lower LUE. In the mean time, no reliable relation was found between the LUE_{NEP} calculated from Eq. (8) and LUE (the figure was not shown here). Therefore, it is feasible to detect LUE_{GPP} with the Fraunhofer Line Principle.

3.4 Photosynthesis detection with Vegetation Indices

Vegetation indices (VIs) could reflect various plant physiological and non-physical information solely from reflection spectra without any other auxiliary data. Accordingly, VIs were widely used in evaluation of vegetation cover and growing

condition qualitatively and quantitatively (Tian *et al.*, 1998). Both solar-induced ChlF and VIs were extracted from canopy reflected spectrum. Several VIs relating to vegetation cover and photosynthesis (Table 1) were chosen to analysis the relation between these VIs and the parameters such as PAR, NEP, GPP and LUE_{GPP}, in order to confirm the advantage of ChlF in vegetation photosynthesis detection.

Many studies have declared good correlation between pho-

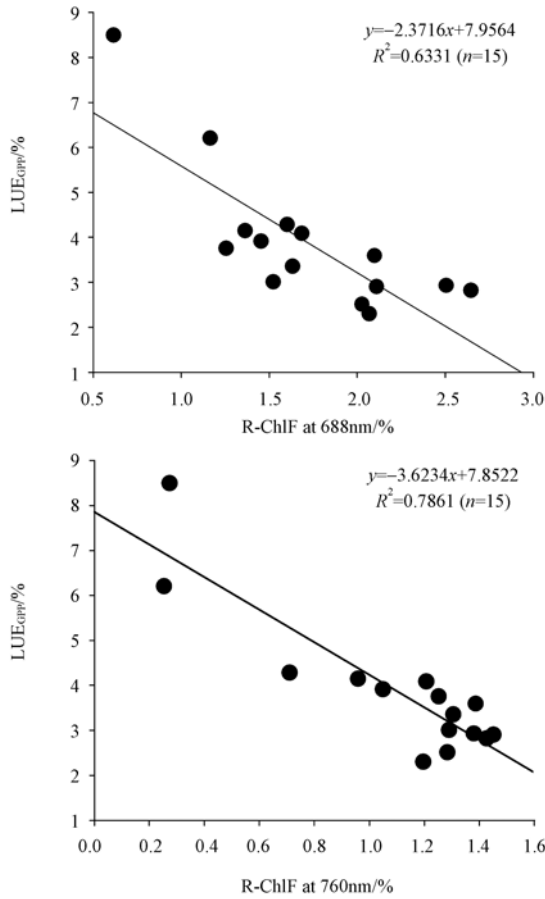


Fig. 7 Relationship between LUE_{GPP} and relative chlorophyll fluorescence (R-ChlF) at 688nm and 760nm

Table 1 Summary of the Vegetation Indices

Vegetation Index	Definition	Source
NDVI	$\frac{R_{800} - R_{680}}{R_{800} + R_{680}}$	Lichtenthaler <i>et al.</i> (1996)
SIPI	$\frac{R_{800} - R_{445}}{R_{800} - R_{680}}$	Penuelas <i>et al.</i> (1995)
PRI	$\frac{R_{531} - R_{570}}{R_{531} + R_{570}}$	Gamon (1992)
CUR	$\frac{R_{683}^2}{R_{675} \times R_{690}}$	Zarco-Tejada <i>et al.</i> (2000)
CARI	$CAR \times \frac{R_{700}}{R_{670}}$	Kim <i>et al.</i> (1994)

R: Reflectance; $CAR = \frac{a \times 670 + R_{670} + b}{(a^2 + 1)^{0.5}}$, $a = \frac{R_{700} - R_{550}}{150}$, $b = R_{550} -$

$a \times 550$

tochemical reflectance index (PRI) and LUE (Chen *et al.*, 2008), which was reconfirmed by the correlation coefficients (R^2) shown in Table 2. All these VIs could not establish reliable correlation with other photosynthesis parameters. Oppositely, combination of vegetation ChlF and R-ChlF could retrieve PAR and CO₂ assimilation rate as well as follow short-time LUE_{GPP} change. The result showed that solar-induced ChlF was more applicable and reliable in LUE detection compared with other VIs.

Table 2 Coefficients of determination (R^2) between Vegetation Indices and photosynthetic parameters

	NDVI	SIPI	PRI	CUR	CARI
PAR	0.0034	0.0001	0.3777	0.0663	0.4068
NEP	0.0002	0.0019	0.2592	0.0101	0.3137
GPP	0.0044	0.0127	0.1503	0.0001	0.2957
LUE _{GPP}	0.0232	0.0848	0.7108	0.0635	0.3792

4 CONCLUSIONS AND DISCUSSIONS

Remote-sensing monitoring of vegetation productivity is a research focus in global climatic change. Benefited from the advantage of large-scale remote-sensing monitoring, LUE-based vegetation productivity models were widely used in monitoring and evaluation of regional agricultural and forestry ecosystems even global ecosystem. As an important input parameter of these LUE-based models, the precision of LUE determines the potential application of the models. Due to the difficulty in LUE detection using remote sensing, a diurnal change experiment was designed on maize to detect LUE using vegetation solar-induced ChlF, based on the physiological mechanism connection between them. The experiment acquired canopy radiance spectra and ecosystem net productivity synchronously, and confirmed the feasibility of detecting LUE using vegetation solar-induced ChlF.

The intensity of ecosystem respiration impacts ecosystem GPP calculation. But, GPP and ecosystem respiration can hardly be distinguished directly by eddy covariance technique. The paper retrieved daytime respiration from empirical exponential model of measured nighttime RE (equal to NEE) and air temperature. This applicable method was adopted in a lot of studies(Wang *et al.*, 2004; Zhang *et al.*, 2007; Yang *et al.*, 2007) under conditions when plant physiologic and biochemical parameters were hard to achieve. Coops *et al.* (2007) reported that since the EC method derives daytime respiration using nighttime flux-temperature relationships ignoring the reduction caused by photo inhibition in leaf respiration in light relative to darkness, thus, the EC method tends to overestimate GPP.

The R-ChlF retrieved from Fraunhofer Line Principle, to a certain extent, can eliminate the influence of incident light energy on the fluorescence intensity, and thus can monitor LUE variation more sensitively. GPP is corresponding to photochemical organism accumulation. And a significantly negative correlation was illustrated between R-ChlF and LUE_{GPP}. In ad-

dition, The VIs, interrelated with vegetation cover and photosynthesis, were calculated, and the correlation between these VIs and the photosynthesis parameters, such as PAR, NEP, GPP and LUE_{GPP} , were analyzed. The results further verified the advantage of ChlF in detection of LUE and other vegetation photosynthesis parameters.

Acknowledgements: The authors gratefully acknowledge financial support provided for this research by the National Basic Research Program of China (973 Program) (2009CB723902) and Western Action Program on Heihe River Remote Sensing Experiment carried out by Chinese Academy of Science. We thank Institute of Remote Sensing Application, Chinese Academy of Science, Cold and Arid Region Environmental and Engineering Research Institute, Chinese Academy of Science, Beijing Normal University and National Engineering Research Center for Information Technology in Agriculture for providing the instruments. Each member is thanked for their assistance in this experiment.

REFERENCES

- Chen J, Tang Y H, Chen X H and Yang W. 2008. The review of estimating light use efficiency through Photochemical Reflectance Index (PRI). *Journal of Remote Sensing*, **12**(2): 331—337
- Coops N C, Black T A, Jassal R S, Trofymow J A and Morgenstern K. 2007. Comparison of MODIS, eddy covariance determined and physiologically modelled gross primary production (GPP) in a Douglas-fir forest stand. *Remote Sensing of Environment*, **107**: 385—401
- Dobrowski S Z, Pushnik J C, Zarco-Tejada P J and Ustin S L. 2005. Simple reflectance indices track heat and water stress-induced changes in steady-state chlorophyll fluorescence at the canopy scale. *Remote Sensing of Environment*, **97**: 403—414
- Evain S, Camenen L and Moya I. 2001. Three channels detector for remote sensing of chlorophyll fluorescence and reflectance from vegetation. 8th International Symposium: Physical Measurements and Signatures in Remote Sensing, Aussois, France, CNES, M. Leroy
- Gamon J A. 1992. A narrow - waveband spectral index that tracks diurnal changes in photosynthetic efficiency. *Remote Sensing of Environment*, **41**: 35—44
- Goulden M L, Munger J W, Fan S-M, Daube B C and Wofsy S C. 1996. Measurements of carbon sequestration by long-term eddy covariance: methods and a critical evaluation of accuracy. *Global Change Biology*, **2**(3): 169—182
- Grace J, Nichol C, Disney M, Lewis P, Quaife T and Bowyer P. 2007. Can we measure terrestrial photosynthesis from space directly, using spectral reflectance and fluorescence? *Global Change Biology*, **13**: 1484—1497
- Hilker T, Coops N C, Wulder M A, Black T A and Guy R D. 2008. The use of remote sensing in light use efficiency based models of gross primary production: A review of current status and future requirements. *Science of The Total Environment*, **404**(2—3): 411—423
- Janzen H H. 2004. Carbon cycling in earth systems—a soil science perspective. *Agricultural, Ecosystems & Environment*, **104**(3): 399—417
- Jenkins J P, Richardson A D, Braswell B H, Ollinger S V, Hollinger D Y and Smith M L. 2007. Refining light-use efficiency calculations for a deciduous forest canopy using simultaneous tower-based carbon flux and radiometric measurements. *Agricultural Forest Meteorology*, **143**: 64—79
- Kim M S, Daughtry C S T, Chappelle E W and McMurtrey J E. 1994. The use of high spectral resolution bands for estimating absorbed photosynthetically active radiation (APAR). Proc. ISPRS'94 Val D' Isere, France
- Law B E, Baldocchi D D and Anthoni P M. 1999. Below canopy and soil CO₂ fluxes in a ponderosa pine forest. *Agricultural and Forest Meteorology*, **94**(3—4): 171—188
- Li C J, Wang J H, Liu L Y and Wang R C. 2004. Automated digital image analyses for estimating percent ground cover of winter wheat based on object features. *Journal of Zhejiang University*, **30**(6): 650—656
- Lichtenthaler H K, Gitelson A A and Lang M. 1996. Nondestructive determination of chlorophylls content of leaves of a green and an aurea mutant of tobacco by reflectance measurements. *Journal of Plant Physiology*, **148**: 483—493
- Liu L Y, Zhang Y J, Wang J H and Zhao C J. 2005. Detecting solar-induced chlorophyll fluorescence from field radiance spectra based on the fraunhofer line principle. *IEEE Transaction on Geoscience and Remote Sensing*, **43**(4): 827—832
- Liu L Y, Zhang Y J, Wang J H and Zhao C J. 2006. Detecting photosynthesis fluorescence under natural sunlight based on fraunhofer line. *Journal of Remote Sensing*, **10**(1): 130—137
- Lloyd J and Taylor J A. 1994. On the temperature dependence of soil respiration. *Functional Ecology*, **8**: 315—323
- Louis J, Ounis A, Ducruet J M, Evain S, Laurila T, Thum T, Aurela M, Wingsle G, Alonso L, Pedros R and Moya I. 2005. Remote sensing of sunlight-induced chlorophyll fluorescence and reflectance of Scots pine in the boreal forest during spring recovery. *Remote Sensing of Environment*, **96**: 37—48
- Moya I, Camenen L, Evain S, Goulas Y, Cerovic Z G, Latouche G, Flexas J and Ounis A. 2004. A new instrument for passive remote sensing 1. Measurements of sunlight-induced chlorophyll fluorescence. *Remote Sensing of Environment*, **91**: 186—197
- Nichol C J, Huemmrich K F, Black A, Jarvis P G, Walthall C L, Grace J and Hall F G. 2000. Remote sensing of photosynthetic-light-use efficiency of boreal forest. *Agricultural and Forest Meteorology*, **101**: 131—142
- Penuelas J, Baret F and Filella I. 1995. Semi-empirical indices to assess carotenoids / chlorophyll a ratio from leaf spectral reflectance. *Photosynthetica*, **31**: 221—230

- Potter C B, Randerson J T, Field C B, Matson P A, Vitousek P M, Mooney H A and Klooster S A. 1993. Terrestrial ecosystem production: a process model based on global satellite and surface data. *Global Biogeochemical Cycles*, **7**(4): 811—841
- Reichstein M, Falge E, Baldocchi D, Papale D, Aubinet M, Berbigier P, Bernhofer C, Buchmann N, Gilmanov T, Granier A, Grunwald T, Havrankova K, Llvesniemi H, Janous D, Knohl A, Laurila T, Lohila A, Loustau D, Matteucci G, Meyers T, Miglietta T, Ourcival J-M, Pumpanen J, Rambal S, Rotenberg E, Sanz M, Tenhunen J, Seufert G, Vaccari F, Vesala T, Yakir D and Valentini R. 2005. On the separation of net ecosystem exchange into assimilation and ecosystem respiration: review and improved algorithm. *Global Change Biology*, **11**(9): 1424—1439
- Running S W, Nemani R, Glassy J M and Thornton P E. 1999. MODIS daily photosynthesis (PSN) and annual net primary production (NEP) product (MOD17), algorithm theoretical basis document. Version 3.0. http://modis.gsfc.nasa.gov/data/dataproducts.php?MOD_NUMBER=17
- Schreiber U, Bilger W and Neubauer C. 1994. Chlorophyll fluorescence as a non-destructive indicator for rapid assessment of in vivo photosynthesis. *Ecological Studies*, **100**(1): 49—70
- Tian Q J and Min X J. 1998. Advances in study on vegetation indices. *Advance in Earth Sciences*, **13**(4): 327—333
- Wang H, Saigusa N, Yamamoto S, Kondo H, Hirano T, Toriyama A and Fujinuma Y. 2004. Net ecosystem CO₂ exchange over a larch forest in Hokkaido, Japan. *Atmospheric Environment*, **38**(40): 7021—7032
- Webb E K, Pearman G I and Leuning R. 1980. Correction of flux measurements for density effects due to heat and water vapour transfer. *Quarterly Journal of the Royal Meteorological Society*, **106**(447): 85—100
- Xiao X M, Zhang Q Y, Hollinger D, Aber J and Moore B. 2005. Modeling gross primary production of an evergreen needle leaf forest using MODIS and climate data. *Ecological Applications*, **15**(3): 954—969
- Yang F, Ichii K, White M A, Hashimoto H, Michaelis A R, Votava P, Zhu A-X, Huete A, Running S W and Nemani R R. 2007. Developing a continental-scale measure of gross primary production by combining MODIS and AmeriFlux data through Support Vector Machine approach. *Remote Sensing of Environment*, **110**: 109—122
- Yuan W, Liu S, Zhou G, Zhou G, Tieszen L L, Baldocchi D, Bernhofer C, Gholz H, Goldstein A H, Goulden M L, Hollinger D Y, Hu Y, Law B E, Stoy P C, Vesala T, Wofsy S C, *et al.* 2007. Deriving a light use efficiency model from eddy covariance flux data for predicting daily gross primary production across biomes. *Agricultural and Forest Meteorology*, **143**: 189—207
- Zarco-Tejada P J, Miller J R, Mohammed G H, Noland T L and Sampson P H. 2000. Chlorophyll fluorescence effects on vegetation apparent reflectance: II. Laboratory and airborne canopy-level measurements with hyperspectral data. *Remote Sensing of Environment*, **74**: 596—608
- Zhang W L, Chen S P, Chen J, Wei L, Han X G and Lin G H. 2007. Biophysical regulations of carbon fluxes of a steppe and a cultivated cropland in semiarid Inner Mongolia. *Agricultural and Forest Meteorology*, **146**: 216—229

冠层光能利用率的叶绿素荧光光谱探测

程占慧^{1,2}, 刘良云¹

1. 中国科学院 对地观测与数字地球科学中心, 北京 100190;

2. 中国农业大学信息与电气工程学院, 北京 100083

摘要: 设计了玉米生长期日变化试验, 同步获取玉米冠层光谱和通量观测数据, 探究从植被发射荧光光谱角度实现植被光能利用率可靠反演的可能性。运用涡度相关法获取群体生态系统净生产力 (NEP), 通过呼吸作用拟合得到冠层总初级生产力 (GPP); 在此基础上结合吸收光合有效辐射 (APAR) 获取冠层光能利用率 (LUE); 同时, 利用叶绿素荧光光谱分离算法, 提取了光合作用叶绿素荧光绝对强度和相对强度。结论表明, 植被发射荧光光谱与光合有效辐射 (PAR) 显著正相关, 760nm 波段荧光与 PAR 的复相关系数 R^2 在 0.99 以上; 叶绿素荧光绝对强度与 NEP 和 GPP 显著正相关, 荧光和 NEP 对环境日变化具有类似的响应特征; 688nm 和 760nm 植被发射的叶绿素荧光相对强度与 LUE_{GPP} 存在可靠负相关关系, 即叶绿素荧光强度越大, 光能利用率越低。同时, 通过比较几种植被指数与各种光合参量的相关性表明, 叶绿素荧光能够更好的跟踪植被光合状态的变化, 更适宜于植被光能利用率的探测。

关键词: 光谱, 叶绿素荧光, 光能利用率, 初级生产力

中图分类号: TP79

文献标识码: A

引用格式: 程占慧, 刘良云. 2010. 冠层光能利用率的叶绿素荧光光谱探测. 遥感学报, 14(2): 356—371

Cheng Z H and Liu L Y. 2010. Estimating light-use efficiency by the separated Solar-induced chlorophyll fluorescence from canopy spectral data. *Journal of Remote Sensing*, 14(2): 356—371

1 引言

每年陆地生态系统通过光合作用能够固定将近 60Gt 的碳, 与此同时地表自养及异养呼吸又将几乎同等数量的碳输送回大气中, 从而完成了地表和大气之间的碳循环过程 (Janzen, 2004)。陆表碳平衡的微小改变可能引起大气中 CO_2 浓度剧烈的变化, 因此遥感尺度上地 - 气碳循环的估算日益成为全球气候变化研究的重点。在众多生产力模型中, 基于光能利用率 (light use efficiency, LUE) 遥感模型由于其计算简便、输入参数少而被广泛地应用于区域乃至全球的生产力估算中 (Potter 等, 1993; Running 等, 1999; Xiao 等, 2005; Hilker 等, 2008)。

光能利用率定义为植被将吸收光能转化成干物质的效率, 是生产力模型的重要输入参数。大尺度 LUE 探测根据地表类型、光、温、水条件等遥感或实测环境参数进行估算, 制约了基于光能利用率生产力模型的发展。涡度相关技术作为目前直接测定

植被与大气间 CO_2 及水热交换的唯一方法, 可以实现冠层水平上 LUE 的直接探测, 并为区域尺度生产力遥感估算提供一条可靠的验证途径。

植被吸收的光能有 3 条去路: 光合作用、热耗散和荧光, 这三者是此消彼长的关系。叶绿素荧光由于其快速、无损伤反映植被光合作用状态的特征, 被誉为光合作用的理想“探针” (Schreiber, 1994), 可用于实时监测植被对光能的利用情况。遥感探测的植被表观反射光谱信号是植被反射的入射光谱信号和植被光合作用发射的荧光信号叠加的结果, 虽然这部分荧光信号十分微弱, 但已有不少研究 (Moya 等, 2004; Liu 等, 2005; Louis 等, 2005; 刘良云等, 2006) 表明运用夫琅和费暗线 (Fraunhofer Lines) 原理可以成功将这部分荧光信号从植被反射光谱中分离出来。迄今为止大部分的工作是围绕主动荧光对光合功能的探测进行, 而被动荧光与自然光照下的植被光合状况的探测还处在初步的研究阶段, 利用被动荧光直接探测植被光能利用率的研究更是鲜见报

收稿日期: 2009-01-05; 修订日期: 2009-05-01

基金项目: 国家 973 项目 (编号: 2009CB723902)、国家自然科学基金项目 (编号: 40771134) 和国家 863 课题 (编号: 2006AA10Z201)。

第一作者简介: 程占慧 (1986—), 女, 硕士研究生, 主要从事植被定量遥感方面的研究。E-mail: zhanhuicheng@163.com

通讯作者: 刘良云, E-mail: lyliu@ceode.ac.cn。

道。因此,本文在荧光与光合作用相关理论的指导下设计日变化试验,获取植被冠层荧光发射光谱,运用涡度相关法观测的通量数据获取了实时光能利用率观测值,在验证荧光与植被初级生产力相关关系的基础上,初步探究利用植被发射荧光光谱探测植被群体光能利用率的可行性,从而为冠层乃至区域尺度上的光能利用率探测提供一种可靠的遥感反演方法。

2 材料与方法

2.1 试验设计

以夏玉米(*summer maize*)为试验对象,设计日变化试验,获取玉米冠层光谱、辐射以及通量数据。试验于 2008-07-05 在甘肃省张掖市盈科灌区(38.85°N, 100.41°E)进行,此时玉米处于大喇叭口期,平均株高为 1.76m。根据李存军等(2004)提供的方法,运用垂直冠层拍摄的数码照片提取出植被覆盖度约为 95%。试验地块面积约为 3.3 hm²,玉米种植与管理模式一致,长势均匀,通量观测塔位于地块中央。当日天气晴朗无云,光合有效辐射在 200—2000 μmol m⁻² s⁻¹ 之间,风速小于 1.5 m s⁻¹。

2.2 冠层光谱测量

试验采用 ASD FieldSpec FR 光谱仪获取玉米冠层光谱,从 10:00—16:00 每隔 1h 测定一次,16:00—20:00 加密为每 0.5h 测定一次。该光谱仪视场角 FOV 为 25°,光谱范围为 350—2500nm。350—1000nm 采样间隔为 1.4nm,光谱分辨率为 3nm,1000—2500nm 采样间隔为 2nm,光谱分辨率为 10nm。光谱测量方式如图 1,将观测架中心转轴固定在竖直方向,顶端水平悬杆南北向放置,并将光

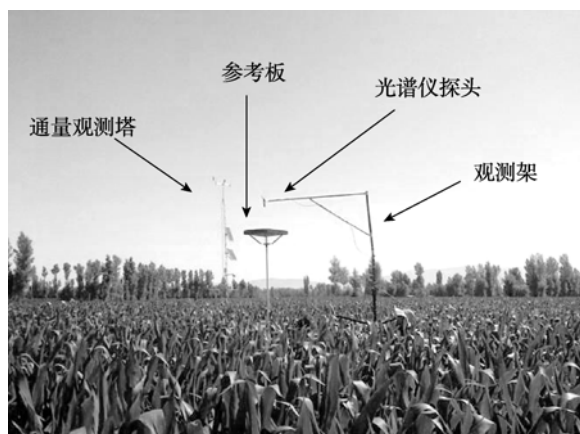


图 1 冠层光谱测量照片

谱仪探头垂直向下固定在悬杆南端,距植被冠层约 2.3m。试验采用 0.5m × 0.5m 灰板作为参考板,在可见光近红外区域的反射率在 45% 左右。试验中参考板用支架托起,其中心点所在垂线与悬杆北端延长线相交,与竖轴水平距离等于悬杆长度,到悬杆垂直距离约 0.5m。

观测采用 Radiance 值模式,试验中每次对目标采样 10 次取平均,并在测定目标后迅速将观测架竖轴旋转 180° 到参考板正上方获取参考板反射辐射亮度值,测定完成后将竖轴再次旋转 180° 到达原先冠层光谱测定位置,尽量保持观测目标的唯一性。

2.3 光合有效辐射测定

试验采用英国 Delta 公司生产的 SunScan 冠层分析系统(SunScan Canopy Analysis System),测量到达冠层顶部的光合有效辐射(Photosynthetic Active Radiation, PAR)、冠层反射的 PAR、到达地表的 PAR 和地表反射的 PAR 共 4 部分。测量时面向南方,将传感器南北向放置,利用手柄处气泡控制探头在测量时始终保持水平状态。在测定冠层顶部 PAR 时,探头距冠层顶部约 20cm,选取地块中 3 处代表性区域分别测定取平均,计算玉米群体光合有效辐射吸收系数。

根据 Jenkins 等(2007)的文献,植被冠层吸收的光合有效辐射(Absorbed Photosynthetically Active Radiation, APAR)可以用式(1)表达:

$$APAR = PAR_i - PAR_r - PAR_t + PAR_g \quad (1)$$

式中, PAR_i, PAR_r, PAR_t, PAR_g 分别表示到达冠层顶部、冠层反射、冠层透射以及地表反射的 PAR。

2.4 通量/气象数据获取

在试验地块架设了一套涡度相关观测系统以及一台自动气象站,用于获取当地气象条件数据并观测地表与近地层大气之间的物质和能量交换,本文利用这两套系统获取了 2008-07-05 的通量和气象观测资料。

此观测站点开路涡度相关系统主要由三维超声风速仪(CAST3, Campbell Scientific Inc., 美国)和红外 CO₂/H₂O 分析仪(LI-7500, Li-Cor. Inc., 美国)组成。数据采集频率为 10Hz,通量数据用采集器实时进行 WPL 校正(Webb 等, 1980),得到 30min 数据产品,包括 CO₂ 通量、潜热和显热通量以及动量通量等。通量方向由下向上时取正值,在生成 30min 产品前由程序自动剔除了不合理的或仪器故障、天气突变等原因产生的野点。同时用自动气象站获取了每日温度、风速、光照等环境参数,间隔为 10min。

3 结果与分析

3.1 植被冠层发射荧光提取

自然光下植被吸收光子后重新发射的荧光与植被反射光谱是叠合在一起的, 仅占到反射能量的3%以下(Grace 等, 2007), 如何有效地从反射光谱中提取植被发射荧光具有重要意义。基于夫琅和费暗线原理的叶绿素荧光光谱分离算法, 由于其简便易行而成功的应用于某些特定波段的植被发射光谱的研究中(Moya 等, 2004; Liu 等, 2005; Louis 等, 2005; 刘良云等, 2006), Evain 等(2001)、Moya 等(2004)基于该原理研制了相应的荧光光谱探测仪器。

由于太阳和地球大气的吸收, 到达地表的太阳光谱曲线存在许多细小的暗线, 这些暗线被称为夫琅和费暗线, 其波谱宽度普遍在 0.1—10nm 之间, 如 486nm、527nm、589nm、688nm 和 760nm 等。叶绿素荧光光谱分离算法的核心思想是: 在假定夫琅和费暗线附近反射率恒定的基础上, 认为自然光照下短波激发的植被叶绿素荧光能够将这夫琅和费“井”填充到一定程度, 通过对某个特定波长的入射辐亮度光谱和植被反射辐亮度光谱的比较, 获得该波段植被荧光发射辐亮度光谱值, 表达式为:

$$f = \frac{a \times d - c \times b}{a - b} \quad (2)$$

其中 f 代表植被发射的叶绿素荧光强度(Chlorophyll fluorescence, ChlF), a , b 分别表示利用参考板获取的太阳入射辐亮度光谱在夫琅和费暗线中心区及其相邻谱区的强度, c , d 分别表示植被冠层反射辐亮度光谱在夫琅和费暗线中心区及其相邻谱区的强度。利用夫琅和费暗线法不仅能计算植被发射的绝对荧光强度, 还能够计算其相对荧光强度(Relative Chlorophyll Fluorescence, R-ChlF), 即植被发射荧光占入射光能的比例, 如式(3):

$$f^*(\%) = \frac{f}{a} \times 100 = \frac{ad - cb}{a^2 - ab} \times 100 \quad (3)$$

其中 f^* 表示植被发射相对荧光强度, 其他参量含义同式(2)。刘良云等(2006)曾在 ASD 光谱仪探测的基础上, 用式(2)和式(3)成功提取了植被在自然光下 688nm 和 760nm 处的荧光发射光谱, 表明利用该算法获取植被发射荧光光谱是可行的。

试验提取的 688nm 和 760nm 处光合作用叶绿素荧光如图 2。夏玉米(C4 植物)荧光发射光谱呈现出早晚低中午高的特征, 且 688nm 处荧光强度要显著高于 760nm 处荧光强度。这与刘良云等(2006)在研究 C4 植物地锦(别名:爬山虎)时的荧光光谱特征一致, 并均与 C3 植物冬小麦在以上两个波段处荧光发

射光谱特征有明显差异。这表明 C3 和 C4 两种植被类型在 688nm 和 760nm 荧光发射波段可能存在着不同的生理机制, 但不同光合途径与荧光产量之间的机理关系目前尚无明确的解释。

在试验观测对象保持不变的情况下, 环境条件的变化对植被叶绿素荧光发射光谱有主要影响, 其中入射光合有效辐射的变化对植被荧光影响最大。如图 3 所示对两者的线性关系进行统计分析表明,

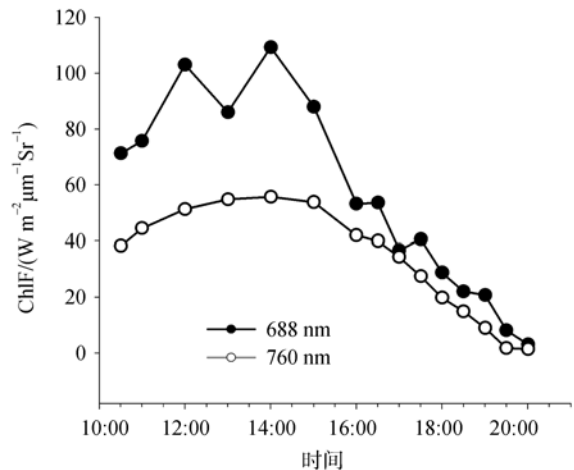


图 2 688 nm 和 760 nm 植被荧光发射辐亮度光谱曲线

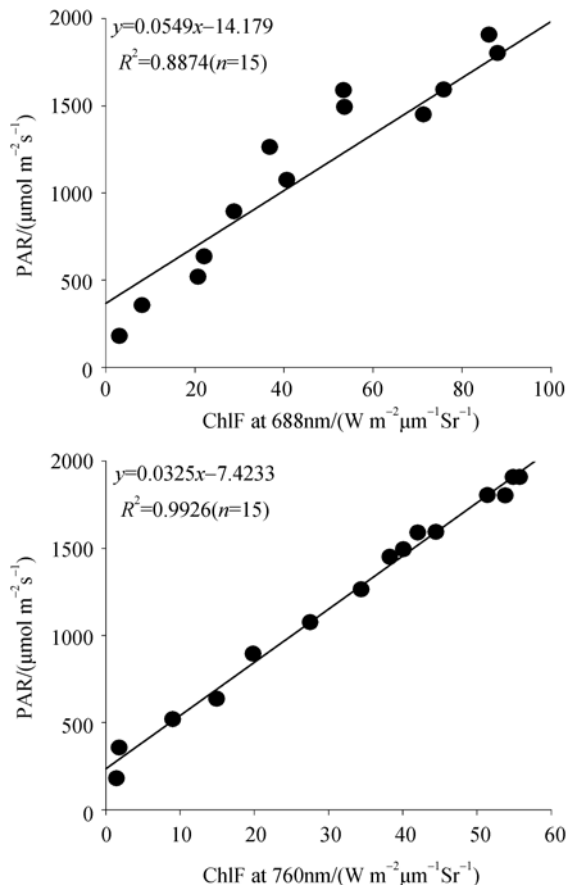


图 3 688 nm 和 760 nm 波段植被荧光发射光谱与光合有效辐射(PAR)相关散点图

688nm 和 760nm 荧光发射光谱与 PAR 均为显著正相关,复相关系数 R^2 分别达到了 0.8874 和 0.9938,这验证了荧光对植被的保护作用,即当光照较强时,植被将更多的光能转换成荧光,避免了过高的光强对植被光合器官的损害。有部分研究(Dobrowski 等,2005; Louis 等, 2005)表明 688nm 处植被发射的荧光会在叶片内部被叶绿素再吸收用于光合作用,这可能是导致图 3 中 688nm 处荧光与 PAR 相关性比 760nm 处相关性低的原因。

3.2 植被初级生产力与荧光绝对强度

3.2.1 生态系统净生产力

涡度相关技术直接观测的是植被/大气间净生态系统 CO_2 交换(Net Ecosystem Exchange, NEE),负值表示生态系统从大气中吸收 CO_2 ,它与生态系统净生产力(Net Ecosystem Production, NEP)绝对值相等但符号相反,即:

$$\text{NEP} = -\text{NEE} \quad (4)$$

本研究采用了定点观测,植被 NEP 和植被发射荧光主要受到了环境因子变化的影响,如图 4, 688nm

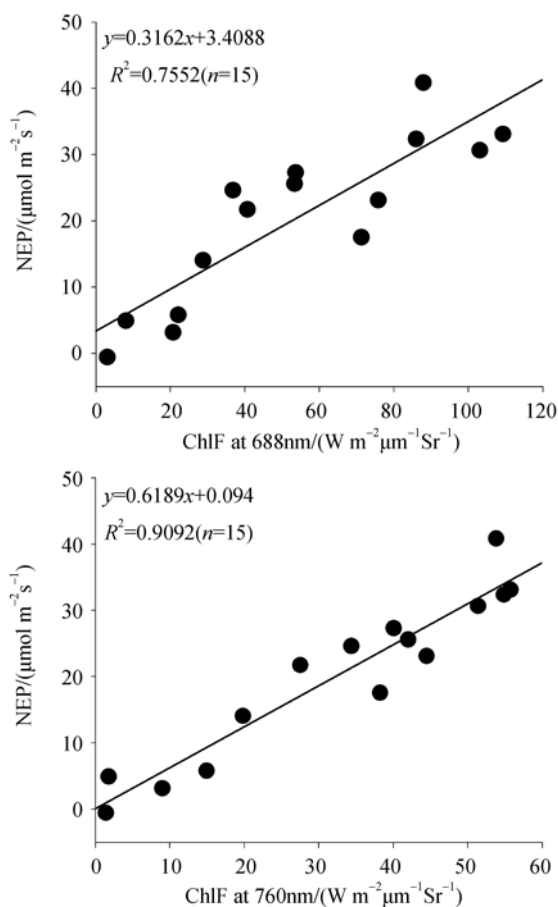


图 4 688 nm 和 760 nm 波段植被荧光发射光谱与生态系统净生产力(NEP)相关散点图

和 760nm 的绝对荧光强度与 NEP 均为显著正相关, R^2 分别为 0.7854 和 0.9279。这表明两者对短期外界环境的变化有相同的响应,在观测对象保持不变的情况下,植被冠层荧光发射光谱能够反映生态系统短期 NEP 变化情况。

3.2.2 总初级生产力

夜间光合作用停止,通量观测系统获取的是生态系统呼吸(Ecosystem Respiration, RE)。大量研究表明温度的指数函数拟合夜间 RE 具有较高的可行性(Lloyd & Taylor, 1994; Nichol 等, 2000; Wang 等, 2004; Zhang 等, 2007)。Reichstein 等(2005)的研究认为土壤温度随深度的增加变化很大,且相比于空气温度拟合的呼吸数据差异较大,因此本文选取气象站获取的 2m 处代替平均气温(T_a)作为拟合公式的自变量,其表达式如式(5):

$$\text{RE} = Ae^{BT_a} \quad (5)$$

式中, A 和 B 是常量,可以通过夜间实测空气温度(T_a)和 CO_2 通量 NEE(即夜间 RE)拟合得到。在假定白天温度对于 RE 的响应与夜晚相同的条件下,可以根据式(5)外推白天生态系统的呼吸(Zhang 等, 2007)。另外,在使用夜间碳通量数据进行呼吸系数的拟合时,考虑到夜间大气湍流稳定状态下 CO_2 通量观测值偏低(Goulden 等, 1996; Law 等, 1999)以及样本数量的限制,本文仅选取了 2008-07-04 到 2008-07-09 之间夜间摩擦风速(Friction velocity, u^*)大于 0.15ms^{-1} 的值(Zhang 等, 2007),排除了剩余约 70%的夜间数据。拟合后得到常量 A 和 B 分别为 2.8898 和 0.0591 ($R^2=0.4703$, $n=15$),并结合式(5)和日间空气温度计算了白天生态系统呼吸量。

不同的生态系统之间呼吸作用对 CO_2 通量交换的影响有较大差异,总初级生产力(Gross Primary Production, GPP)表征的是在没有任何呼吸消耗情况下植被光合作用固碳的总量,根据文献(Wang 等, 2004; Yuan 等, 2007; Coops 等, 2007)GPP 可以用 NEP 与 RE 的加和进行表示:

$$\text{GPP} = \text{NEP} + \text{RE} \quad (6)$$

GPP、NEP、RE 的日变化曲线如图 5,全天植被呼吸 RE 占 GPP 值在 30% 以上,并在早晚 NEP 较低时该比例分别上升到了 77% 和 100%。同时,对图 5 数据积分得到 CO_2 气体交换在三者之间的分配比例为 $\text{GPP}:\text{NEP}:\text{RE}=0.5:0.3:0.2$,这些表明呼吸作用对植被光合固碳量的消耗不可忽略。特别是在傍晚 18:00 之后地表温度仍维持在较高水平时,NEP 迅速下降到零值附近,此时 GPP 仍保持在 $13.58\mu\text{mol m}^{-2} \text{s}^{-1}$ 的较高水平,表明此时植被自养呼吸占据主导地位,

光合作用制造有机碳量不足以抵扣生态系统呼吸消耗碳量。

植被发射荧光也正是植被光合状态的表观体现,不与呼吸作用直接关联,因此讨论冠层荧光发射强度与植被群体总初级生产力之间的相关关系更具备生理意义。图6给出了688nm和760nm处绝对对荧光

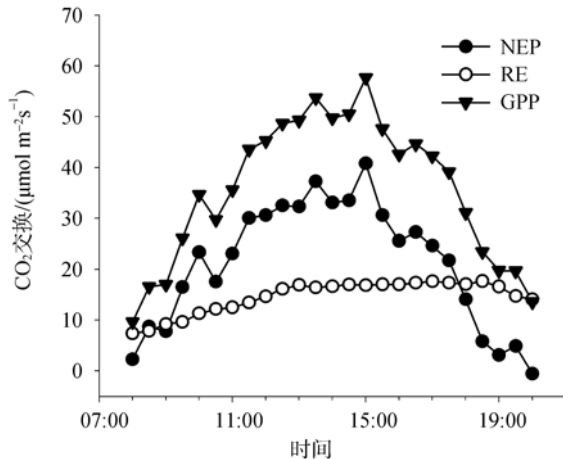


图5 生态系统净生产力(NEP)、总初级生产力(GPP)和生态系统呼吸(RE)日变化曲线图

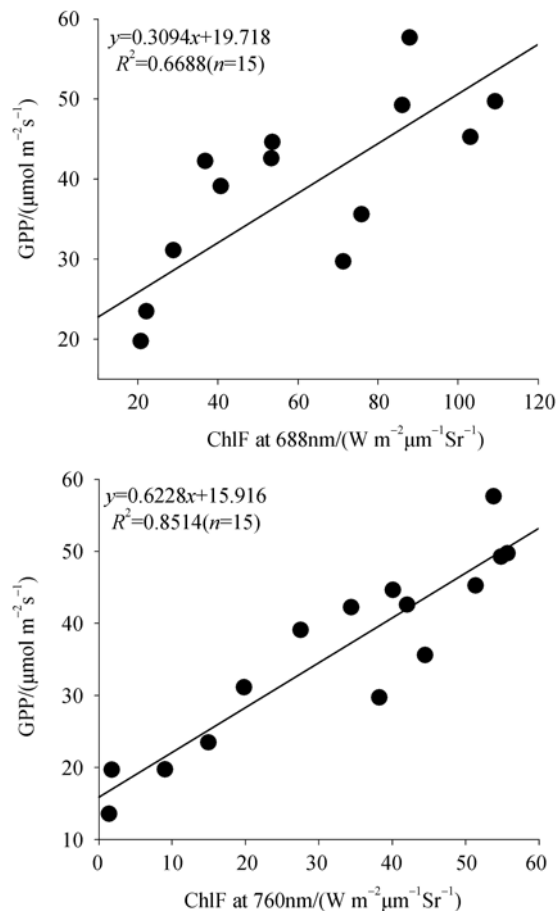


图6 688 nm 和 760 nm 波段植被荧光发射光谱与总初级生产力(NEP)相关散点图

强度与 GPP 的统计关系,研究表明荧光与 GPP 之间显著正相关,复相关系数 R^2 分别为 0.6688(688nm)和 0.8514(760nm)。

图4和图6共同表明植被发射荧光光谱与植被群体 NEP 和 GPP 之间均存在显著正相关关系,尤其是在 760nm 波段复相关系数均达到了 0.85 以上,说明利用植被发射荧光探测植被光能利用率具备一定的可行性。

3.3 光能利用率与荧光相对强度

通常,光能利用率(Light use efficiency, LUE)的计算如下,

$$LUE(\%) = \frac{P}{APAR} \times 100 \quad (7)$$

式中, APAR 为植被吸收的光合有效辐射并由式(1)计算得到, P 根据 LUE 模型计算输出参数的不同可以有不同的表示方法,本文根据实测通量数据分别计算了基于 NEP 的光能利用率(LUE_{NEP})和基于 GPP 的光能利用率(LUE_{GPP}),表达式见式(8)。

$$LUE_{NEP}(\%) = \frac{NEP}{APAR} \times 100 \quad (8)$$

$$LUE_{GPP}(\%) = \frac{GPP}{APAR} \times 100$$

植被发射荧光和 GPP 是光合作用过程的直接产物,荧光与植被呼吸作用没有直接的生理关联。因此将植被通过光化学反应固定有机碳总量作为光能利用率计算的输入参数,消除了生态系统呼吸对光合固碳消耗的影响,叶绿素荧光与 LUE_{GPP} 之间的物理机制更直接,根据式(8)分别计算了 LUE_{NEP} 和 LUE_{GPP} 。

式(3)定义的叶绿素荧光相对强度与 LUE 换算机理相吻合,因此可以更加敏感地追踪植被光能利用率日变化情况。图7分别给出了688nm和760nm相对荧光强度与 LUE_{GPP} 的统计关系,表明荧光相对强度与 LUE_{GPP} 之间存在负相关关系, R^2 分别为 0.6331 和 0.7861,即植被发射荧光越强植被光能利用率越低。同时统计了 LUE_{NEP} 与相对荧光强度的相关关系,结论显示两者之间不能建立可靠的负相关关系(图略)。因此利用夫琅和费暗线原理探测基于 GPP 的植被光能利用率是可行的。

3.4 植被指数对光合作用的探测

植被指数(Vegetation indices, VIs)只通过光谱信号而不需要其他的辅助资料来实现对植物状态信息的表达,因而广泛地应用于定性和定量的评价植被覆盖及其生长活力中(田庆久等,1998)。植被荧光和植被指数是从植被反射光谱中提取出来,本文选择

了几个与植被覆盖和光合作用相关的植被指数(表 1)与 PAR、NEP、GPP 和 LUE_{GPP} 进行相关分析, 研究植被发射荧光在光合作用探测上的优越性。

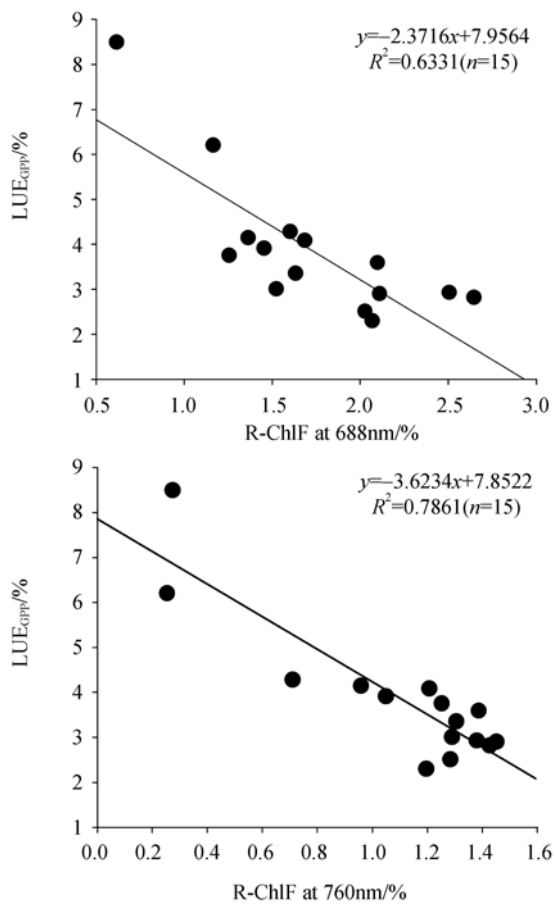


图 7 688 nm 和 760 nm 波段荧光相对强度(R-ChlF)与光能利用率(LUE_{GPP})相关散点图

表 1 植被指数列表

植被指数	定义	出处
NDVI	$\frac{R_{800} - R_{680}}{R_{800} + R_{680}}$	Lichtenthaler 等 (1996)
SIPI	$\frac{R_{800} - R_{445}}{R_{800} - R_{680}}$	Penuelas 等(1995)
PRI	$\frac{R_{531} - R_{570}}{R_{531} + R_{570}}$	Gamon(1992)
CUR	$\frac{R_{683}^2}{R_{675} \times R_{690}}$	Zarco-Tejada 等 (2000)
CARI	$CAR \times \frac{R_{700}}{R_{670}}$	Kim 等(1994)

注: R 为反射率; $CAR = \frac{|a \times 670 + R_{670} + b|}{(a^2 + 1)^{0.5}}$, $a = \frac{R_{700} - R_{550}}{150}$, $b = R_{550} - a \times 550$

很多研究表明光化学植被指数(Photochemical Reflectance Index, PRI)与 LUE 有良好的相关性(陈晋等, 2008), 表 2 中给出的植被指数与光合参数的相

关性(R^2)也证实了这一点。但这些植被指数不能建立起与其他光合作用参数的相关关系, 植被绝对和相对荧光强度的结合不仅能跟踪短期 LUE_{GPP} 的变化, 还能够较好地反演光照和 CO_2 同化速率的变化情况。这表明相比于其他植被指数, 植被自然光下发射的荧光更适宜于光能利用率的可靠探测。

表 2 植被指数与光合作用参数相关性

	NDVI	SIPI	PRI	CUR	CARI
PAR	0.0034	0.0001	0.3777	0.0663	0.4068
NEP	0.0002	0.0019	0.2592	0.0101	0.3137
GPP	0.0044	0.0127	0.1503	0.0001	0.2957
LUE_{GPP}	0.0232	0.0848	0.7108	0.0635	0.3792

4 结论与讨论

植被生产力遥感监测是全球气候变化的研究重点, 基于光能利用率的植被生产力监测模型由于其大尺度上的监测优势, 被普遍应用于区域农林生态系统甚至全球生态系统的监测和评价中。光能利用率作为该模型的重要输入参数, 其数值输入的精确度直接影响了模型应用潜力。鉴于自然光照条件下植被发射荧光与光能利用率之间的机理联系, 本文针对遥感监测中光能利用率难以直接获取的出发点设计日变化试验, 同步获取了植被冠层荧光发射光谱、生态系统净生产力以及植被光能利用率的日变化情况, 初步验证应用自然光下植被发射荧光探测植被光能利用率的可行性。

呼吸作用的强弱对植被 GPP 估算影响很大, 利用涡度相关的方法不能直接区分生态系统光合固碳和呼吸消耗这两个部分, 本文采用的方法是通过夜间气温与通量数据拟合并外推得到白天生态系统呼吸分量。在其他植被生理生化参数获取困难的情况下, 利用夜间涡度拟合的方法外推日间生态系统呼吸由于其简单易行而被众多文献采用(Wang 等, 2004; Zhang 等, 2007; Yang 等, 2007), 但 Coops 等(2007)的研究指出用该方法没有考虑到日间高温高光强对植被呼吸的抑制作用, 估算日间 GPP 值可能偏高。

根据夫琅和费暗线原理获取了植被发射荧光相对强度, 在一定程度上消除了光照条件对荧光发射强度的影响, 能够更加敏感地追踪光能利用率变化情况。由于植被光合作用物质积累对应的是 GPP, 利用自然光下荧光发射光谱探测基于 GPP 的光能利用率具有更可靠的理论基础, 试验结果表明荧光相对

强度与 LUE_{GPP} 有较好的负相关关系。另外, 本文运用获取的冠层反射光谱提取了与植被光合、覆盖相关的植被指数, 并与光合作用参数进行相关分析, 进一步验证了荧光在光能利用率及其他光合参数探测上的优越性。

致谢 实验工作是在国家重点基础研究发展计划(973)项目(2009CB723902)和中国科学院西部行动计划(二期)联合实施的“黑河综合遥感联合实验”的支持下完成的, 在此表示感谢。感谢中国科学院遥感应用研究所、中国科学院寒区旱区环境与工程研究所、北京师范大学、国家农业信息化工程技术研究中心提供的仪器观测设备和人员协助。感谢参与本次实验的所有老师和同学!

REFERENCES

- Chen J, Tang Y H, Chen X H and Yang W. 2008. The review of estimating light use efficiency through Photochemical Reflectance Index (PRI). *Journal of Remote Sensing*, **12**(2): 331—337
- Coops N C, Black T A, Jassal R S, Trofymow J A and Morgenstern K. 2007. Comparison of MODIS, eddy covariance determined and physiologically modelled gross primary production (GPP) in a Douglas-fir forest stand. *Remote Sensing of Environment*, **107**: 385—401
- Dobrowski S Z, Pushnik J C, Zarco-Tejada P J and Ustin S L. 2005. Simple reflectance indices track heat and water stress-induced changes in steady-state chlorophyll fluorescence at the canopy scale. *Remote Sensing of Environment*, **97**: 403—414
- Evain S, Camenen L and Moya I. 2001. Three channels detector for remote sensing of chlorophyll fluorescence and reflectance from vegetation. 8th International Symposium: Physical Measurements and Signatures in Remote Sensing, Aussois, France, CNES, M. Leroy
- Gamon J A. 1992. A narrow - waveband spectral index that tracks diurnal changes in photosynthetic efficiency. *Remote Sensing of Environment*, **41**: 35—44
- Goulden M L, Munger J W, Fan S-M, Daube B C and Wofsy S C. 1996. Measurements of carbon sequestration by long-term eddy covariance: methods and a critical evaluation of accuracy. *Global Change Biology*, **2**(3): 169—182
- Grace J, Nichol C, Disney M, Lewis P, Quaife T and Bowyer P. 2007. Can we measure terrestrial photosynthesis from space directly, using spectral reflectance and fluorescence? *Global Change Biology*, **13**: 1484—1497
- Hilker T, Coops N C, Wulder M A, Black T A and Guy R D. 2008. The use of remote sensing in light use efficiency based models of gross primary production: A review of current status and future requirements. *Science of The Total Environment*, **404**(2—3): 411—423
- Janzen H H. 2004. Carbon cycling in earth systems: a soil science perspective. *Agricultural, Ecosystems & Environment*, **104**(3): 399—417
- Jenkins J P, Richardson A D, Braswell B H, Ollinger S V, Hollinger D Y and Smith ML. 2007. Refining light-use efficiency calculations for a deciduous forest canopy using simultaneous tower-based carbon flux and radiometric measurements. *Agricultural Forest Meteorology*, **143**: 64—79
- Kim M S, Daughtry C S T, Chappelle E W and McMurtrey J E. 1994. The use of high spectral resolution bands for estimating absorbed photosynthetically active radiation (APAR). Proc. ISPRS'94 Val D' Isere, France
- Law B E, Baldocchi D D and Anthoni P M. 1999. Below canopy and soil CO₂ fluxes in a ponderosa pine forest. *Agricultural and Forest Meteorology*, **94**(3—4): 171—188
- Li C J, Wang J H, Liu L Y and Wang R C. 2004. Automated digital image analyses for estimating percent ground cover of winter wheat based on object features. *Journal of Zhejiang University*, **30**(6): 650—656
- Lichtenthaler H K, Gitelson A A and Lang M. 1996. Nondestructive determination of chlorophylls content of leaves of a green and an aurea mutant of tobacco by reflectance measurements. *Journal of Plant Physiology*, **148**: 483—493
- Liu L Y, Zhang Y J, Wang J H and Zhao C J. 2005. Detecting solar-induced chlorophyll fluorescence from field radiance spectra based on the fraunhofer line principle. *IEEE Transaction on Geoscience and Remote Sensing*, **43**(4): 827—832
- Liu L Y, Zhang Y J, Wang J H and Zhao C J. 2006. Detecting photosynthesis fluorescence under natural sunlight based on fraunhofer line. *Journal of Remote Sensing*, **10**(1): 130—137
- Lloyd J and Taylor J A. 1994. On the temperature dependence of soil respiration. *Functional Ecology*, **8**: 315—323
- Louis J, Ounis A, Ducruet J M, Evain S, Laurila T, Thum T, Aurela M, Wingsle G, Alonso L, Pedros R and Moya I. 2005. Remote sensing of sunlight-induced chlorophyll fluorescence and reflectance of Scots pine in the boreal forest during spring recovery. *Remote Sensing of Environment*, **96**: 37—48
- Moya I, Camenen L, Evain S, Goulas Y, Cerovic Z G, Latouche G, Flexas J and Ounis A. 2004. A new instrument for passive remote sensing 1. Measurements of sunlight-induced chlorophyll fluorescence. *Remote Sensing of Environment*, **91**: 186—197
- Nichol C J, Huemmrich K F, Black A, Jarvis P G, Walthall C L, Grace J and Hall F G. 2000. Remote sensing of photosynthetic-light-use efficiency of boreal forest. *Agricultural and Forest Meteorology*, **101**: 131—142
- Penuelas J, Baret F and Filella I. 1995. Semi-empirical indices to assess carotenoids / chlorophyll a ratio from leaf spectral reflectance. *Photosynthetica*, **31**: 221—230
- Potter C B, Randerson J T, Field C B, Matson P A, Vitousek P M, Mooney H A and Klooster S A. 1993. Terrestrial ecosystem production: a process model based on global satellite and surface data. *Global Biogeochemical Cycles*, **7**(4): 811—841
- Reichstein M, Falge E, Baldocchi D, Papale D, Aubinet M, Berbigier P, Bernhofer C, Buchmann N, Gilmanov T, Granier A, Grunwald T, Havrankova K, Ilvesniemi H, Janous D, Knohl A, Laurila T, Lohila A, Loustau D, Matteucci G, Meyers T, Migli-

- etta T, Ourcival J-M, Pumpanen J, Rambal S, Rotenberg E, Sanz M, Tenhunen J, Seufert G, Vaccari F, Vesala T, Yakir D and Valentini R. 2005. On the separation of net ecosystem exchange into assimilation and ecosystem respiration: review and improved algorithm. *Global Change Biology*, **11**(9): 1424—1439
- Running S W, Nemani R, Glassy J M and Thornton P E. 1999. MODIS daily photosynthesis (PSN) and annual net primary production (NEP) product (MOD17), algorithm theoretical basis document. Version 3.0. http://modis.gsfc.nasa.gov/data/dataproduct/dataproducts.php?MOD_NUMBER=17
- Schreiber U, Bilger W and Neubauer C. 1994. Chlorophyll fluorescence as a non-destructive indicator for rapid assessment of in vivo photosynthesis. *Ecological Studies*, **100**(1): 49—70
- Tian Q J and Min X J. 1998. Advances in study on vegetation indices. *Advance in Earth Sciences*, **13**(4): 327—333
- Wang H, Saigusa N, Yamamoto S, Kondo H, Hirano T, Toriyama A and Fujinuma Y. 2004. Net ecosystem CO₂ exchange over a larch forest in Hokkaido, Japan. *Atmospheric Environment*, **38**(40): 7021—7032
- Webb E K, Pearman G I and Leuning R. 1980. Correction of flux measurements for density effects due to heat and water vapour transfer. *Quarterly Journal of the Royal Meteorological Society*, **106**(447): 85—100
- Xiao X M, Zhang Q Y, Hollinger D, Aber J and Moore B. 2005. Modeling gross primary production of an evergreen needle leaf forest using MODIS and climate data. *Ecological Applications*, **15**(3): 954—969
- Yang F, Ichii K, White M A, Hashimoto H, Michaelis A R, Votava P, Zhu A-X, Huete A, Running S W and Nemani R R. 2007. Developing a continental-scale measure of gross primary production by combining MODIS and AmeriFlux data through Support Vector Machine approach. *Remote Sensing of Environment*, **110**: 109—122
- Yuan W, Liu S, Zhou G, Zhou G, Tieszen L L, Baldocchi D, Bernhofer C, Gholz H, Goldstein A H, Goulden M L, Hollinger D Y, Hu Y, Law B E, Stoy P C, Vesala T, Wofsy S C, et al. 2007. Deriving a light use efficiency model from eddy covariance flux data for predicting daily gross primary production across biomes. *Agricultural and Forest Meteorology*, **143**: 189—207
- Zarco-Tejada P J, Miller J R, Mohammed G H, Noland T L and Sampson P H. 2000. Chlorophyll fluorescence effects on vegetation apparent reflectance: II. Laboratory and airborne canopy-level measurements with hyperspectral data. *Remote Sensing of Environment*, **74**: 596—608
- Zhang W L, Chen S P, Chen J, Wei L, Han X G and Lin G H. 2007. Biophysical regulations of carbon fluxes of a steppe and a cultivated cropland in semiarid Inner Mongolia. *Agricultural and Forest Meteorology*, **146**: 216—229

附中文参考文献

- 陈晋, 唐艳鸿, 陈学泓, 杨伟. 2008. 利用光化学反射植被指数估算光能利用率研究的进展. *遥感学报*, **12**(2): 331—337
- 李存军, 王纪华, 刘良云, 王人潮. 2004. 基于数字照片特征的小麦覆盖度自动提取研究. *浙江大学学报*, **30**(6): 650—656.
- 刘良云, 张永江, 王纪华, 赵春江. 2006. 利用夫琅和费暗线探测自然光条件下的植被光合作用荧光研究. *遥感学报*, **10**(1): 130—137
- 田庆久, 闵祥军. 1998. 植被指数研究进展. *地球科学进展*, **13**(4): 327—333